Supplementary Data

Synthesis and application of tuneable carbon-silica composites from the microwave pyrolysis of waste paper for selective recovery of gold from acidic solutions

Konstantina Sotiriou,[a] Nontipa Supanchaiyamat,[b] Tengyao Jiang,[a] Intuorn Janekarn,[b] Andrea Muñoz García,[a] Vitaliy L. Budarin,[a] Duncan J. MacQuarrie[a] and Andrew J. Hunt [b]*

[a] Green Chemistry Centre of Excellence, Department of Chemistry, University of York, Heslington, York, YO10 5DD, UK

[b] Materials Chemistry Research Center, Department of Chemistry and Center of Excellence for Innovation in Chemistry, Faculty of Science, Khon Kaen University, Khon Kaen, 40002, Thailand

*Corresponding authors email: andrew@kku.ac.th

NITROGEN ADSORPTION/ DESORPTION POROSIMETRY

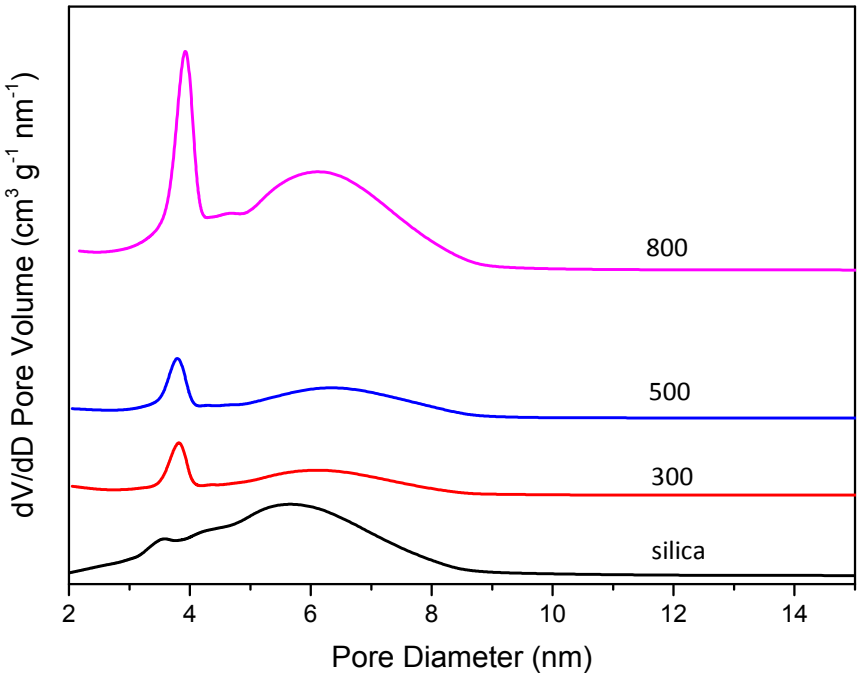

Fig. S1 Pore size distribution curves of silica gel K60 and CSCs

INFRARED DATA

Table S1 Adsorption bands observed in IR spectra of CSCs

Functional Group	**Characteristic Adsorption**	**Notes**
O-H stretch	3200-3550 cm^{-1}	Due to the presence of carboxylic acids
Alkyl C-H stretch	2950-2850 cm^{-1}	Aliphatic chains of bio-oil
C=O stretch	1790-1680 cm^{-1}	Due to the presence of carboxylic acids, esters, ketones, aldehydes.
Si-O-Si asymmetric stretch	1150-100 cm^{-1}	Due to interaction of silanol groups and bio-oil.
Si-O-Si symmetric stretch	900-700 cm^{-1}	Due to interaction of silanol groups and bio-oil.

X-RAY PHOTOEMISSION SPECTROSCOPY DATA

Table S2 Carbon nature and corresponding binding energies for peak deconvolution of C1s spectra of CSCs

Carbon Nature	**Binding Energy/ eV**
C=C sp^2	284-284.6
C-C sp^3	284.6-285.1
C- O (C-O-C, C-O-H)	285.5-286.9
C=O	287.1-287.7
C-O-Si	288-290

Table S3 Gold nature and corresponding binding energies for peak deconvolution of Au4f spectra of CSCs

Element	Nature	Binding Energy / eV
Au (4f 7/2)	Au(0)	84.2 ± 0.4
Au (4f 5/2)	Au(0)	87.9 ± 0.4
Au (4f 7/2)	Au(I)	85.8 ± 0.4
Au (4f 5/2)	Au(I)	86.2 ± 0.4
Au (4f 7/2)	Au(III)	86.4 ± 0.2
Au (4f 5/2)	Au(III)	90.1 ± 0.2

Au4f XPS Spectra

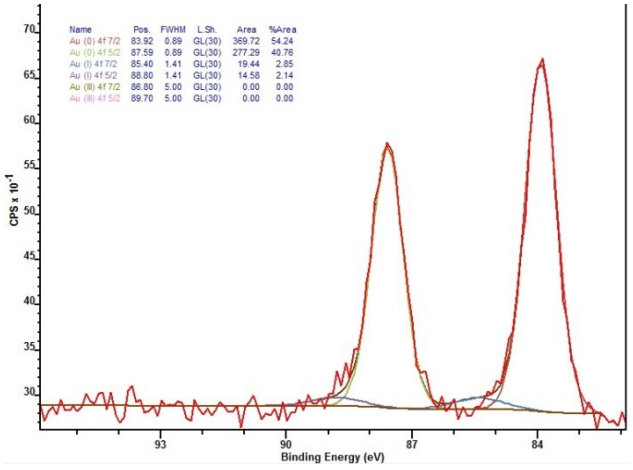

Fig. S2 Au4f spectrum for CSC300 after adsorption in 300 mg L^{-1} of $AuCl_3$

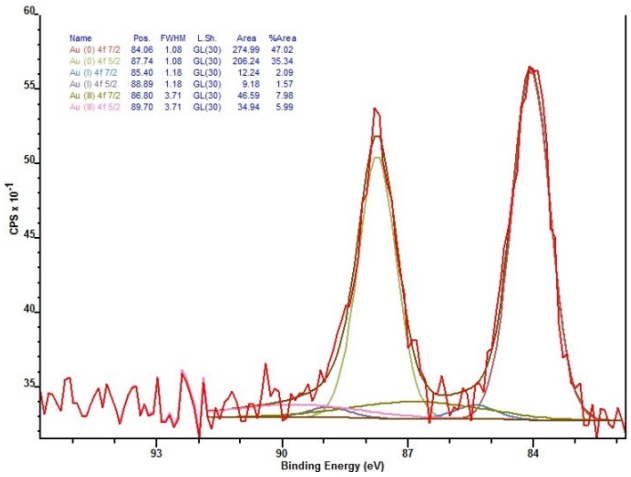

Fig. S3 Au4f spectrum for CSC300 after adsorption in 50 mg L^{-1} of $AuCl_3$

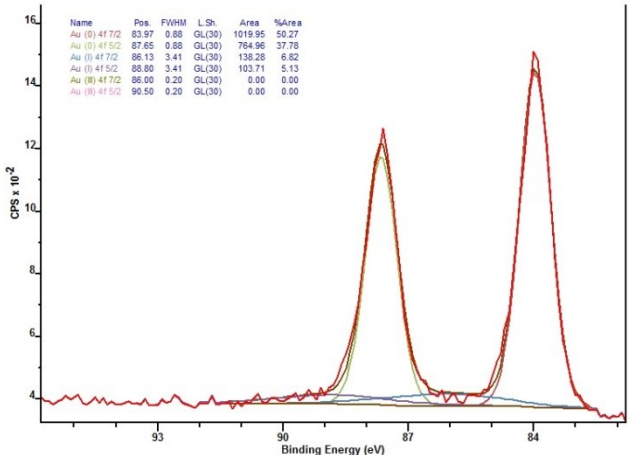

Fig. S4 Au4f spectrum for CSC500 after adsorption in 500 mg L^{-1} of $AuCl_3$

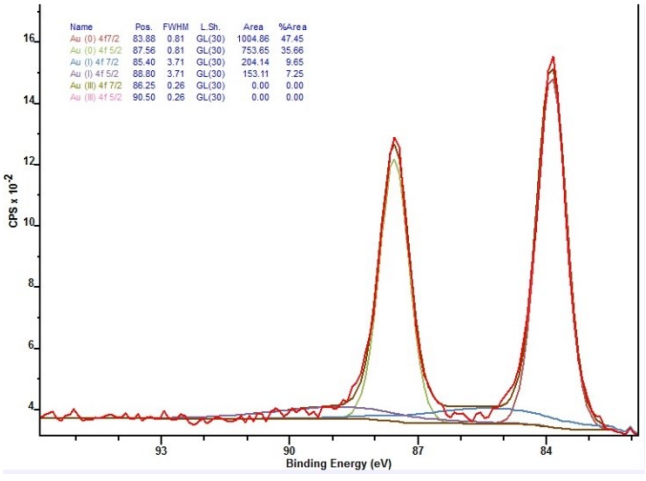

Fig. S5 Au4f spectrum for CSC500 after adsorption in 300 mg L^{-1} of $AuCl_3$

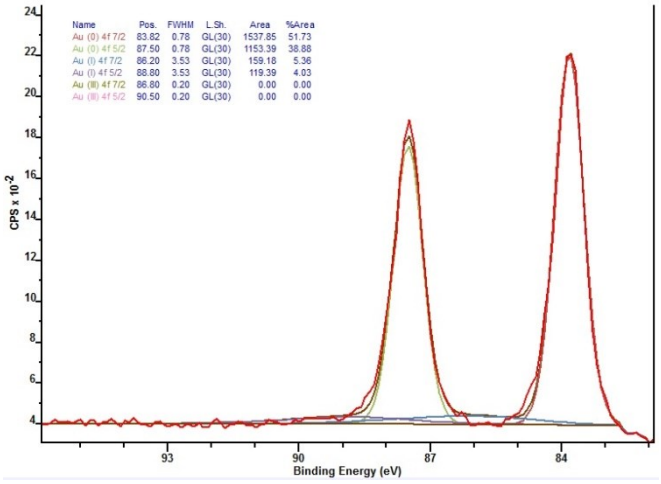

Fig. S6 Au4f spectrum for CSC500 after adsorption in 100 mg L^{-1} of $AuCl_3$

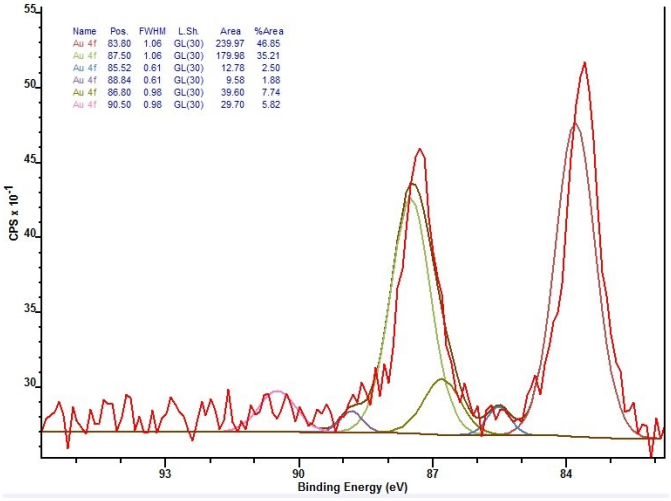

Fig. S7 Au4f spectrum for CSC500 after adsorption in 50 mg L^{-1} of $AuCl_3$

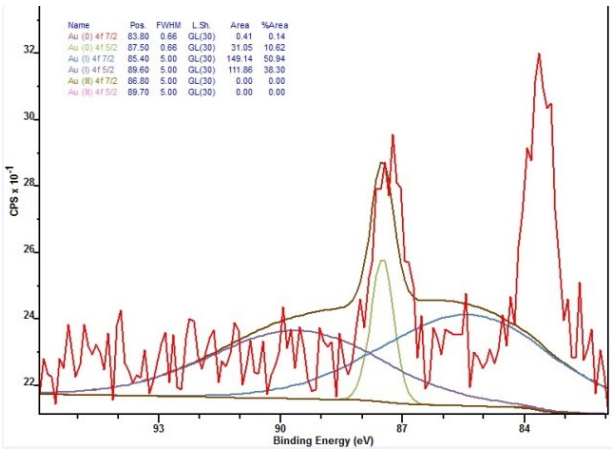

Fig. S8 Au4f spectrum for CSC800 after adsorption in 300 mg L^{-1} of $AuCl_3$

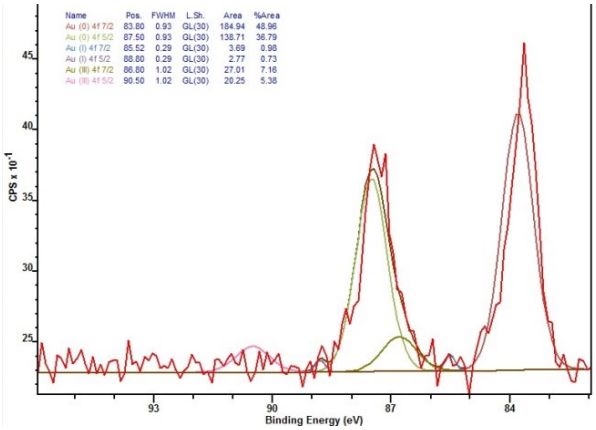

Fig. S9 Au4f spectrum for CSC800 after adsorption in 50 mg L^{-1} of $AuCl_3$

POWDER X-RAY DIFFRACTION

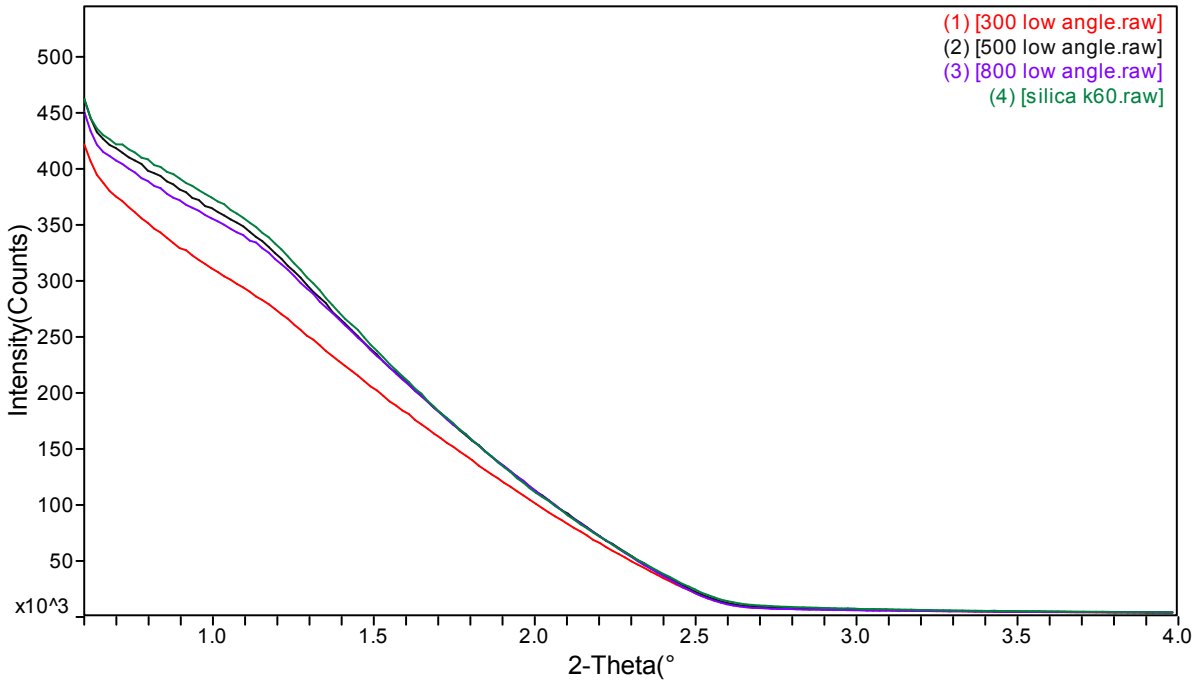

Fig. S10 Small Angle XRD patterns of silica gel K60 and CSCs

SCANNING ELECTRON MICROSCOPY- ENERGY DISPERSIVE X-RAY ANALYSIS

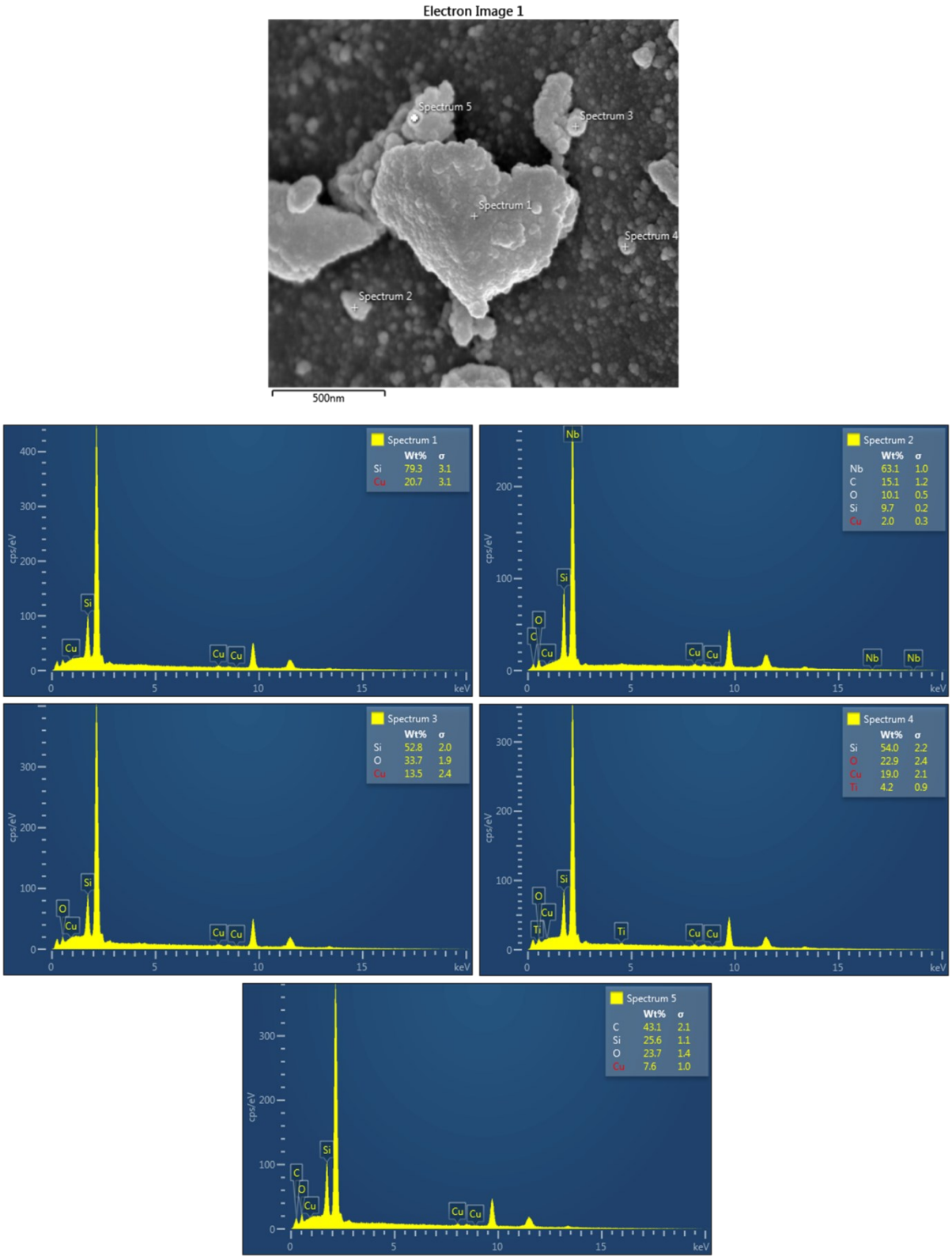

Fig. S11 SEM- EDX of CSC300

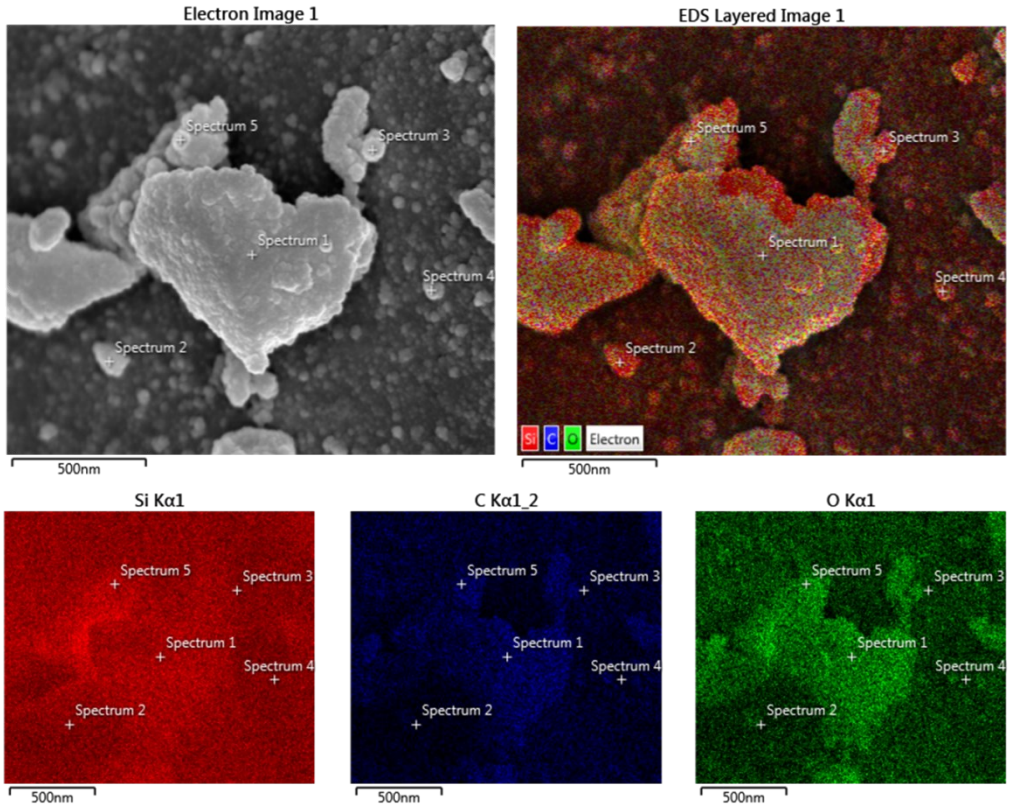

Fig. S12 SEM- EDX mapping of C, Si and O for CSC300

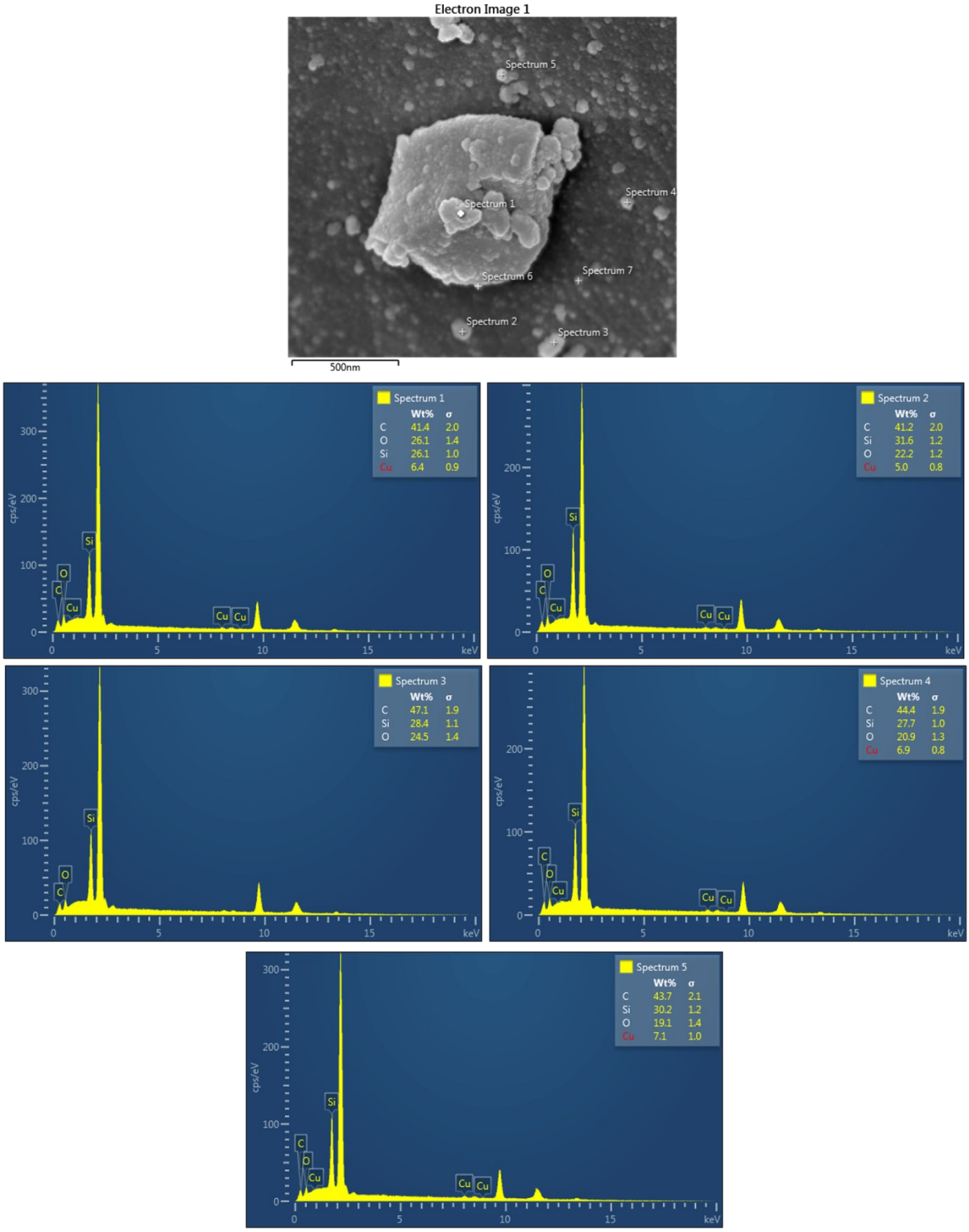

Fig. S13 SEM- EDX of CSC500

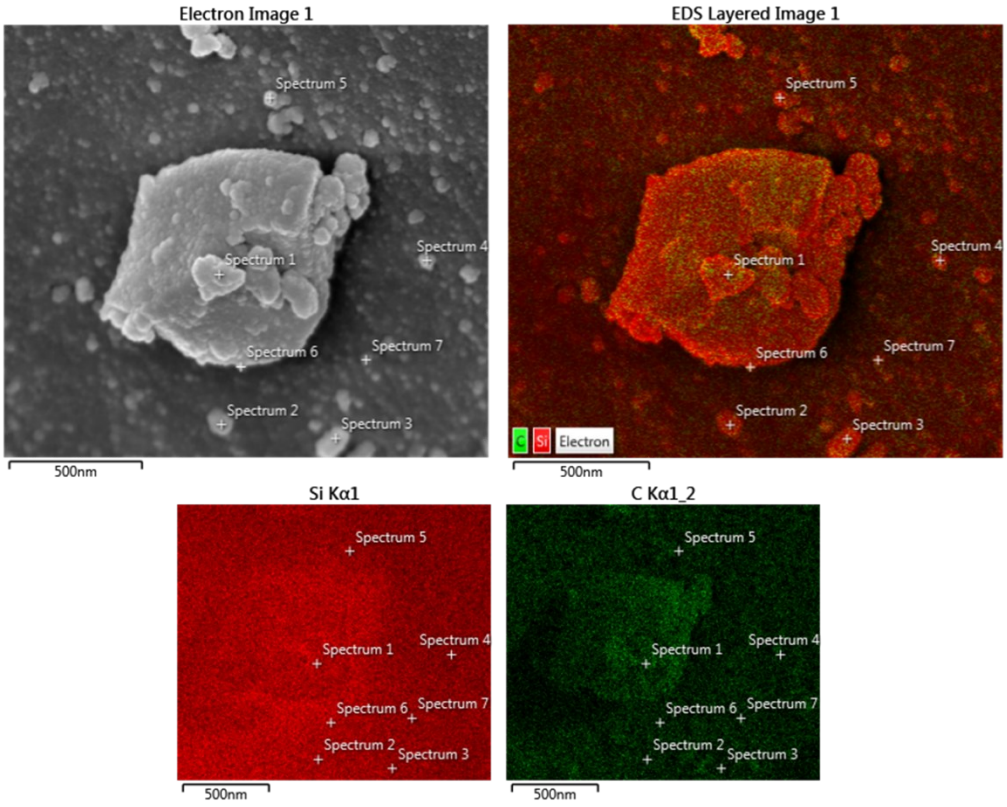

Fig. S14 SEM- EDX mapping of C and Si for CSC500

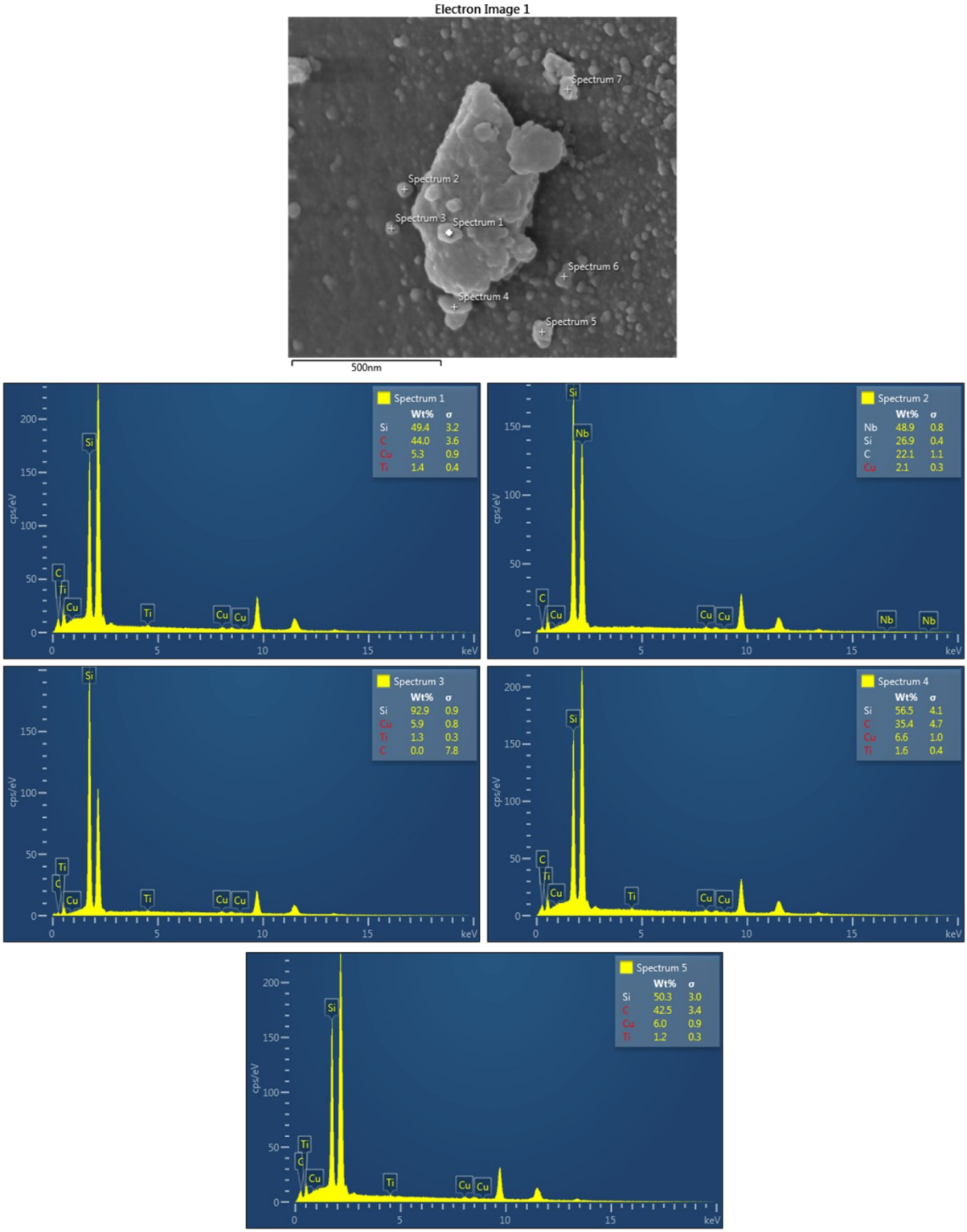

Fig. S15 SEM- EDX of CSC800

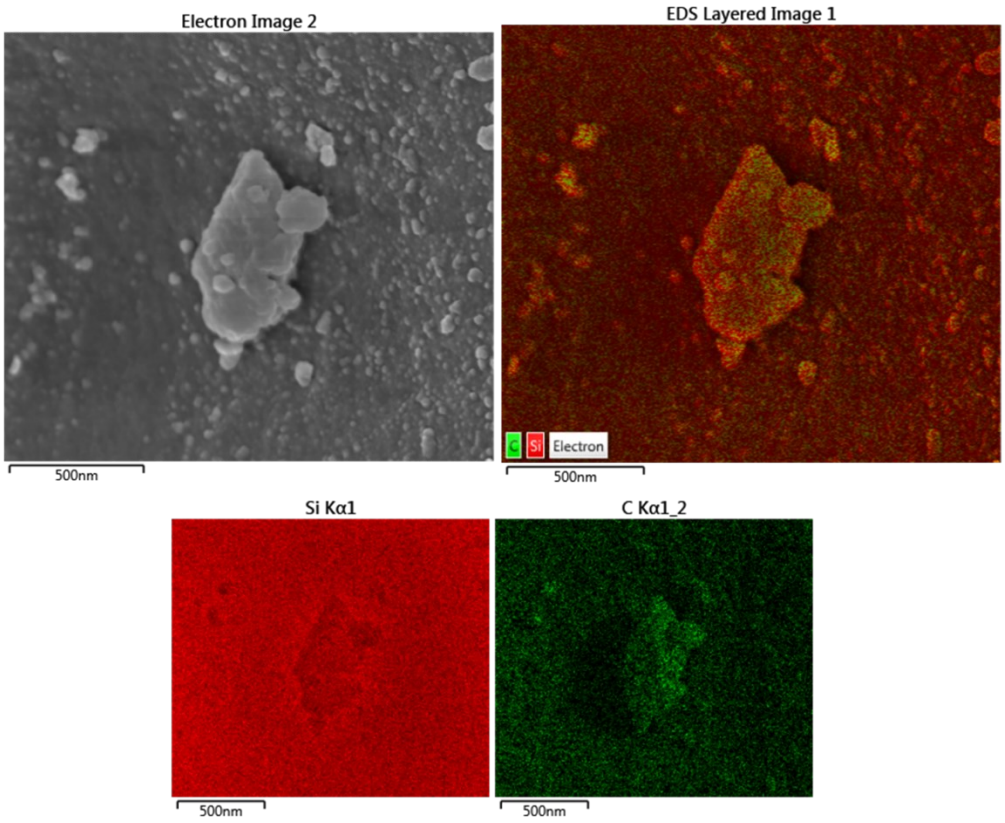

Fig. S16 SEM- EDX mapping of C and Si for CSC800

GOLD ADSORPTION DATA

Gold Selectivity of CSCs

Linear model fittings: Langmuir model

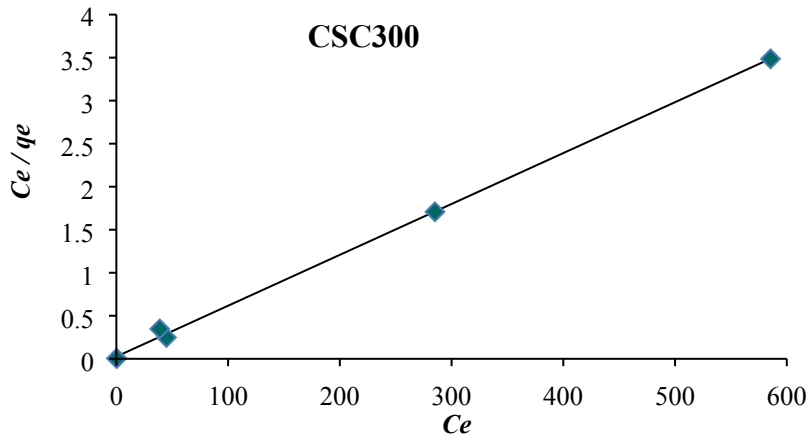

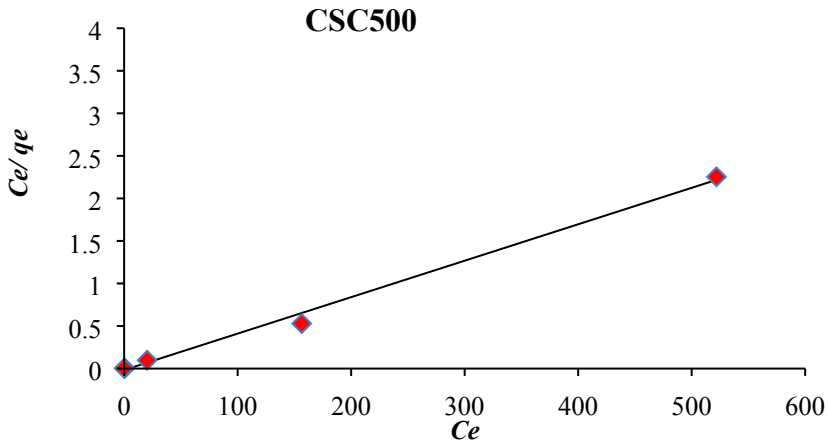

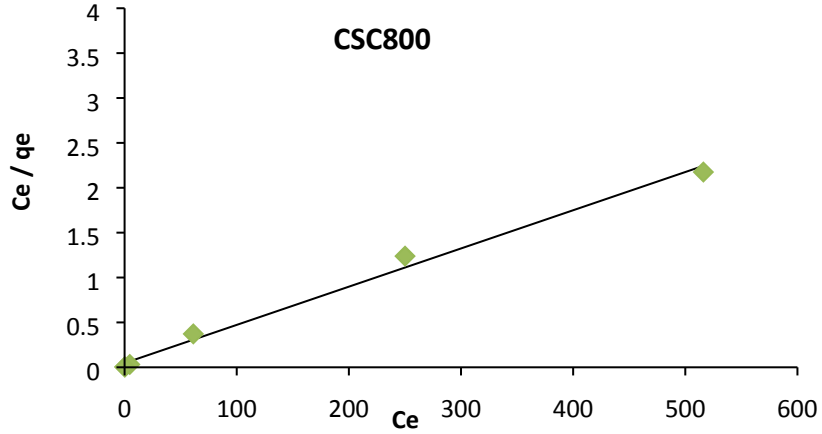

Linear model fittings: Freundlich model

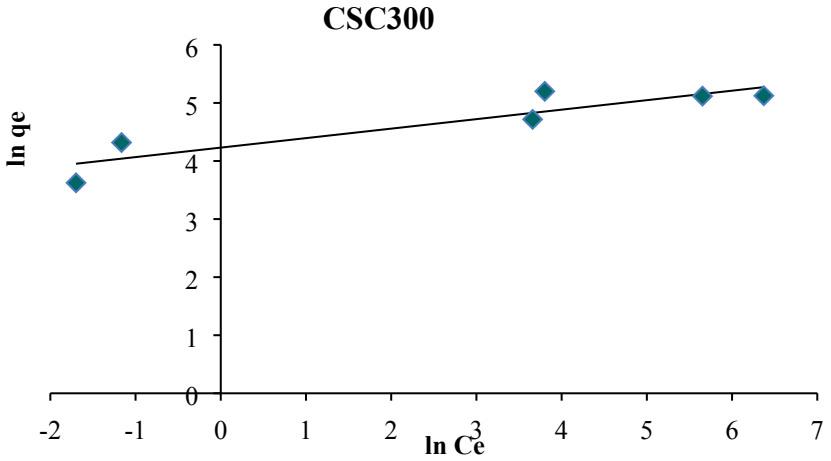

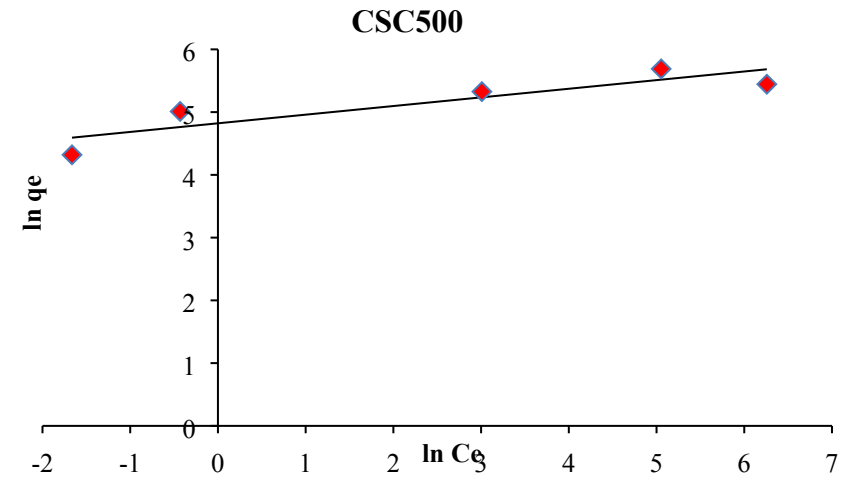

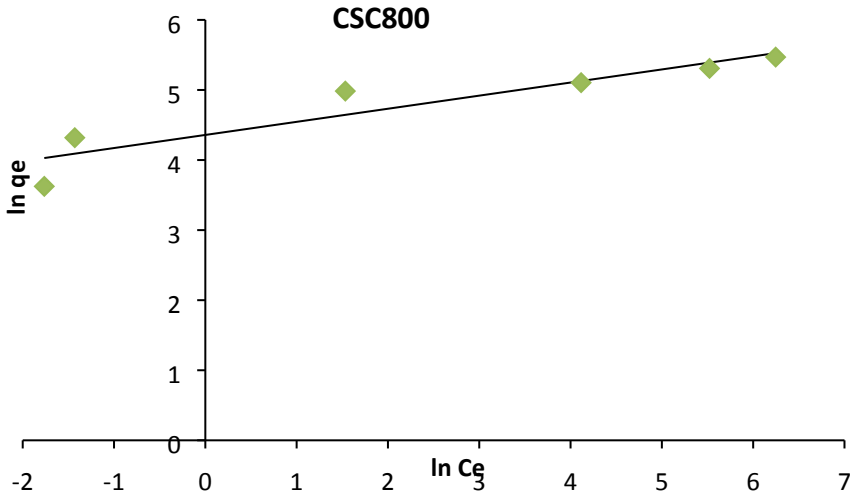

Linear model fittings: D-R model

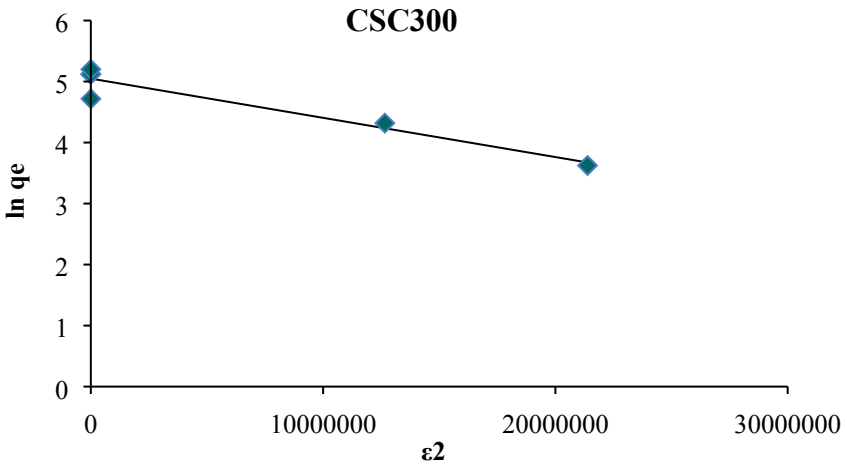
CSC300
ln qe
6
5
4
3
2
1
0
0
10000000
20000000
30000000
ε2

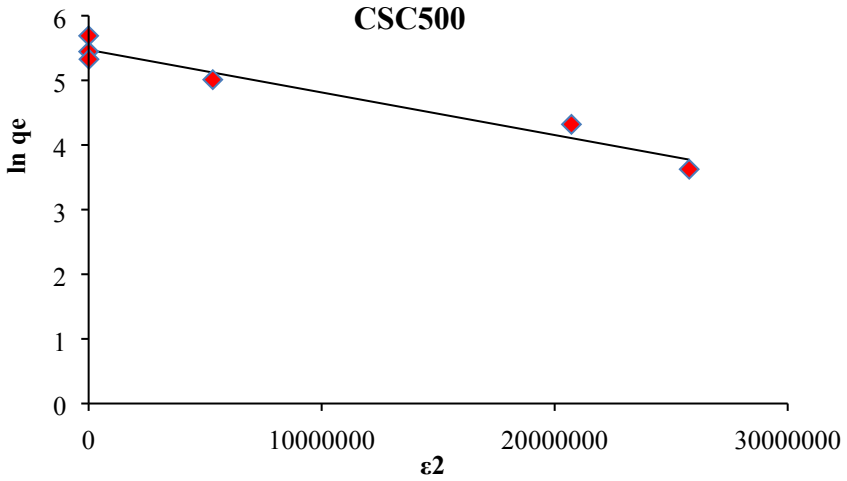
CSC500
ln qe
6
5
4
3
2
1
0
0
10000000
20000000
30000000
ε2

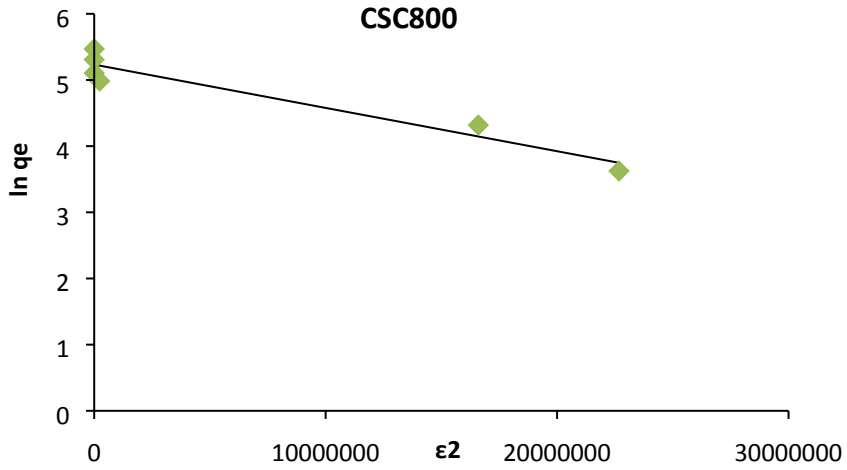
CSC800
ln qe
6
5
4
3
2
1
0
0
10000000
ε2
20000000
30000000

MICROWAVE PYROLYSIS SETUP